Int. J. Electrochem. Sci., 10 **(2015)** 529 - 537

International Journal of
ELECTROCHEMICAL
SCIENCE
www.electrochemsci.org

Short Communication

Graphene/ Magnetite Nanocomposite for Potential Environmental Application

Mohamed A. Farghali[1], *Taher A. Salah El-Din*[1,*], *Abdullah M. Al-Enizi*[2], *Ramadan M. El Bahnasawy*[3]

[1]Nanotechnology and Advanced Materials Central lab, Agriculture Research Center PO Box 588 Orman, Giza, Egypt.
[2]Chemistry Department, College of Science, King Saud University, PO Box 2455, Riyadh 11451, Riyadh, Kingdom of Saudi Arabia.
[3]Chemistry Department, Faculty of Science, Menofiya University, Egypt.
[*]E-mail: t1salah@hotmail.com

Received: 2 October 2014 / *Accepted:* 11 November 2014 / *Published:* 2 December 2014

The application of nanomaterials in water treatment has attracted significant attention recently. graphene/Fe_3O_4 nanocomposites (G/Fe3O4) with different ratios were prepared by solvothermal method and characterized using X-ray diffraction (XRD), high resolution transmission electron microscope (HR-TEM), vibrating sample magnetometer (VSM), and X-ray photoelectron spectroscopy (XPS), The effect of the composition ratios on the removal of methylene blue dye (MB) from aqueous solutions was investigated.

Keywords: Wastewater treatment; Methylene blue removal; Adsorption; Graphene/Fe_3O_4nanocomposite; Magnetic separation.

1. INTRODUCTION

Environmental pollution as a result of rapid development of technologies is one of the serious global concerns [1]. Industrial wastewater is one of the most important pollution sources in the pollution of the water environment [2]. Dye wastewater discharged from industries such as dye synthesis, electroplating, leather, pulp mill, paper, printing, food, cosmetic and textile are major sources of contamination responsible for the continuous water pollution [3-6]. Nowadays, Nanotechnolgy has been used in many applications includes energy [7,8], industrial [9], sensors [10] and environmental applications [11]. It provided fast and effective solution of many challenging problems that cannot be dealt with using conventional technologies [12]. The electrochemical catalytic performance of graphene has also proved a high efficiency related to specific applications such as

energy devices, supercapacitorsand electrochemical sensors [13-15]. With its high surface area, the adsorption capacity of materials based grapheme for dyes or some other organic matters has been reported [16-18]. On the other hand, magnetic composites including graphene, graphene oxide and iron oxide have been used in removing organic dyes from polluted water [19-23].

In this context, the main task of this study is to show the effect of the composition ratios of magnetic nanocomposite (G/Fe3O4) on the removal of methylene blue dye (MB) from aqueous solutions.

2. EXPERIMENTAL

2.1. Materials

All chemicals used in this investigation were of analytical grade and used without further purification treatment. Graphite powder (C, -200 mesh, 99.9999% - Alfa Aesar), sulfuric acid (H_2SO_4, 95–97%, Sigma–Aldrich), sodium nitrate ($NaNO_3$, 99.5%, Sigma), potassium permanganate($KMnO_4$, 99.0%,Sigma–Aldrich), hydrogen peroxide(H_2O_2, 32%, Alfa Aesar), anhydrous iron (III) chloride ($FeCl_3$, 97%,Sigma–Aldrich), ethylene glycol ($C_2H_6O_2$, 99.5%, Sigma), sodium acetate anhydrous ($C_2H_3NaO_2$, 99.0%, Sigma–Aldrich), hydrochloric acid (HCl, 38%,Sigma–Aldrich),sodium hydroxide pellets anhydrous (NaOH, 98%,Sigma–Aldrich), ethyl alcohol (C_2H_5OH, 99.5%, Sigma–Aldrich) and MB ($C1_6H_{18}ClN_3S.2H_2O$, Rankem).

2.2. Synthesis of GO

Graphene oxide (GO) was synthesized using the modified Hummers' method [24] through oxidation of graphite powder. Briefly, 2 g of Sodium nitrate was added into 100 mL of sulfuric acid, followed by stirring at 70 ^oC for 30 min. After that 2 g of graphite powder was added to the mixture, followed by stirring at 70 ^oC for 45 minutes. Subsequently, the mixture was kept below 5^oC in ice bath, and then 12 g of potassium permanganate was slowly added into the mixture. After being heated to 35 ^oC, the mixture was stirred for another five hours until became very viscous reddish green paste. After that, 184 mL of deionized water was added to the above mixture during a period of 30 min, and then the mixture was kept at 98 ^oC for another one hour. Finally, 560 mL of hot deionized water and 20 mL of 5% hydrogen peroxide were added into the mixture to stop the reaction. After the mixture was centrifuged and washed with 10% hydrochloric acid solution for several times to remove the residual metal ions. The powder was dried at 60 ^oC under vacuum condition to get the brown GO sheets.

2.3. Synthesis of graphene/ magnetite nanocomposite (G/Fe3O4)

Synthesis of G/Fe3O4 nanocomposite material was carried out using a solvothermal method [23]. In atypical experiment,5.0 g Sodium acetate was dissolved in a susbended solution of GO (500 mg)/ 80 mL ethylene glycol. After that, 0.42 g $FeCl_3$was added into the solution with stirring and in

presence of nitrogen gas flow to prevent the oxidation of iron. And then, prepared mixture was sealed in a teflon-lined stainless steel autoclave and kept at 200 ^{o}C for 10 h, then cooled to room temperature. Produced materials was washed several times with Ethanol/deionized water for several times, and dried overnight in vacuum oven at 60 ^{o}C.The same above experiment obtained pure G and pure magnetite NPs without using ferric chloride and GO respectively. Changing the feeding weight ratios of Fe_3O_4 to G (m Fe_3O_4: m G = 0.1:1, 0.2:1, 0.4:1, 0.6:1, 0.8:1 and 1:1), gave six samples of G/Fe3O4 nanocomposites ($S_{0.1}$, $S_{0.2}$, $S_{0.4}$, $S_{0.6}$, $S_{0.8}$ and S_1, respectively).

2.4. Adsorption experiments

Batch adsorption experiments were performed on bench top shaker (Unimax 1010 DT - Heidolph, Germany) with a shaking speed of 350 rpm. Different amounts of G/Fe3O4 nanocomposite were added to 200 ml of various MB concentrations at room temperature. G/Fe3O4 nanocomposite was magnetically separated from the aqueous solution after a specific times using permanent magnet, and the final concentrations of the MB solution was determined as a function of absorbance by preparation calibration curve over the concentration range (0–15 ppm) with maximum absorption wavelength (λ_{max}= 665nm) of the MB using a spectrophotometer.

The equilibrium adsorption capacity (q_e) of the nanoadsorbents can be defined as the equilibrium amount in (mg) of MB adsorbed per unit mass (gram) of adsorbent (simply the unit will be noted as mg/ g), and it was calculated using the general equation [70]:

$$q_e = \frac{(C_o - C_e)V}{M} \quad (1)$$

Where; C_o and C_e represent the MB concentrations before and after equilibrium (mg/L) respectively, V is the volume of the MB solution (L) and M is the mass of the adsorbent used in the reaction mixture (g).

3. RESULTS AND DISCUSSION

3.1 Physical Characterization

Prepared magnetic nanocomposites with different ratios of (G : Fe_3O_4) were examined by TEM, as presented in Figure 1. The TEM images reveal a uniform sheet like shape of prepared graphene and a uniform spherical homogeneously distributed of Fe_3O_4 Nps with no agglomeration over the G sheet with the average particle size of 14 nm. Also the images reveal an increasing of the of Fe_3O_4 Nps on the surface of G sheets by increasing the concentration of $FeCl_3$ salt loading; For the samples of ($S_{0.8}$ and S_1), the Fe_3O_4Nps nearly blocked all active sites of the G sheet.

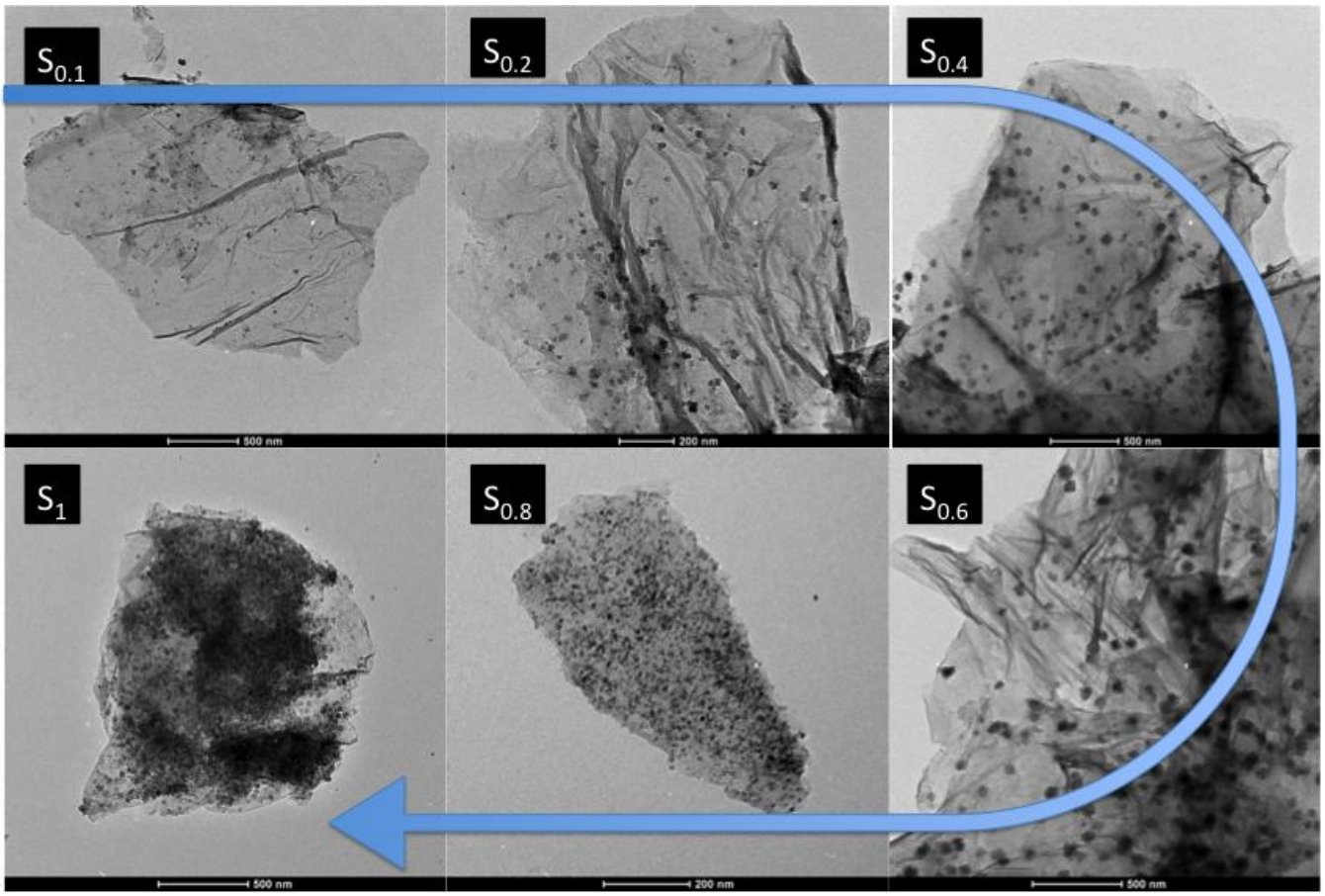

Figure 1. TEM micrographs of the G/Fe3O4 (different ratios: ($S_{0.1}$, $S_{0.2}$, $S_{0.4}$, $S_{0.6}$, $S_{0.8}$ and S_1, respectively).

The XRD patterns for the as-prepared G/Fe3O4 nanocomposites with different ratiosare shown in Figure 2.

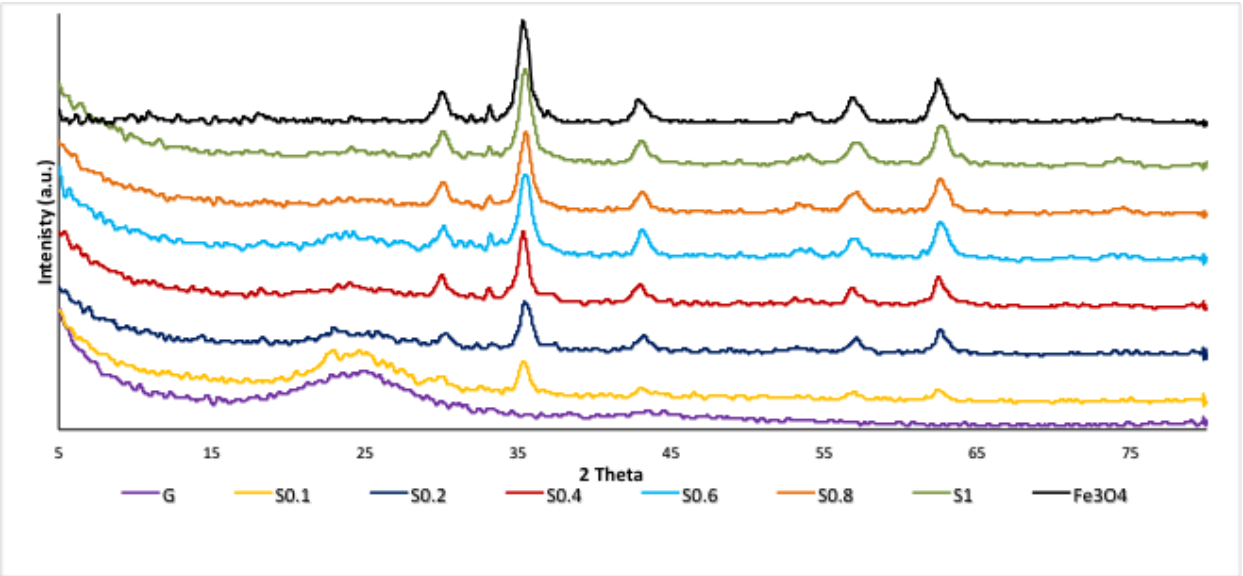

Figure 2. XRD patterns of the graphene, Pure Fe_3O_4, and the G/Fe3O4 (different ratios: ($S_{0.1}$, $S_{0.2}$, $S_{0.4}$, $S_{0.6}$, $S_{0.8}$ and S_1, respectively).

The series of diffraction peaksthat observed at 2θ values of 30.11^{o} (220), 35.47^{o} (311), 43.05^{o} (400), 56.94^{o} (511) and 62.51^{o} (440) in the pattern consistent with the cubic phase spinel structure Fe_3O_4 (JCPDS: No. 04-006-6497).With the increasing thecontent of iron source, the intensity of the five typical reflection peaks of Fe_3O_4(30.1^{o}, 35.4^{o}, 43.05^{o}, 56.94^{o}, and 62.51^{o})was increased. On the other hand, a typical broad peak with an obvious disappearance of the characteristic peaks has been observed with the XRD patterns of graphene nanosheets, which could be attributed to the formation of very thin graphene layers [25].

Figure 3 shows the magnetic hysteresis loops of series of G/Fe3O4 nanocomposite samples($S_{0.1}$, $S_{0.2}$, $S_{0.4}$, $S_{0.6}$, $S_{0.8}$ and S_1). It can be seen that the magnetization increased sharply with the increasing the Fe_3O_4Nps. For the samples($S_{0.1}$, $S_{0.2}$, $S_{0.4}$, $S_{0.6}$, $S_{0.8}$ and S_1) the saturation magnetization (Ms) were(9.0, 18.0, 22.0, 26.0, 36.0, 39.0 emu/g respectively), which are significantly lower than that (80.0 emu/g) measured from a pure Fe_3O_4 NPs [26].

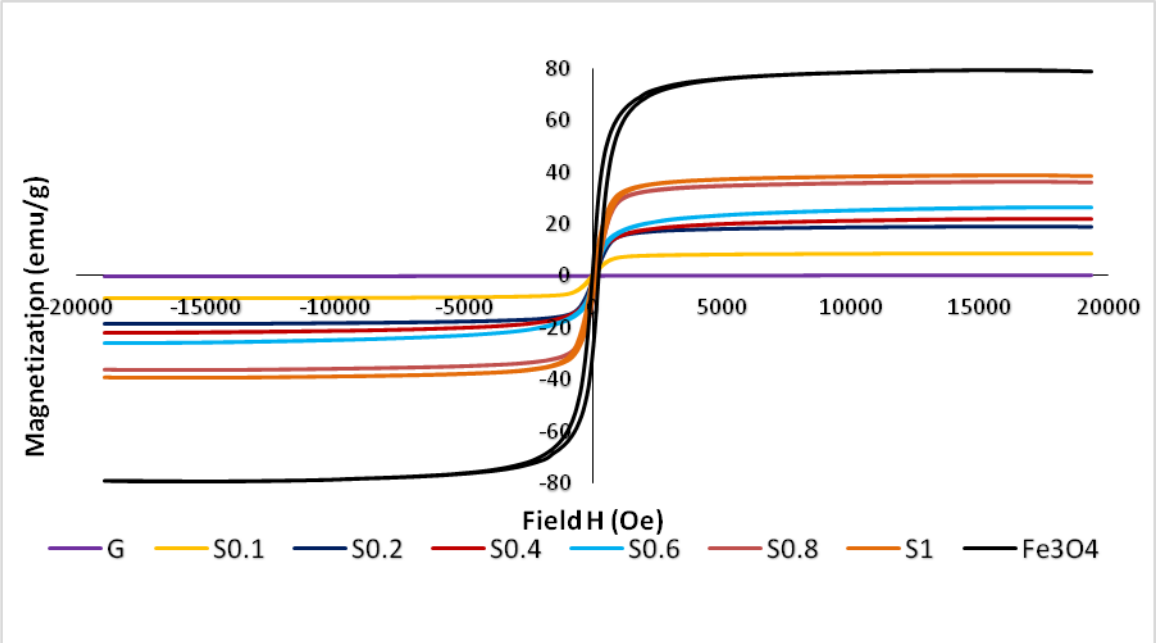

Figure 3. *M-H*curves of pure Graphene, pure Fe_3O_4,and the G/Fe3O4 (different ratios: ($S_{0.1}$, $S_{0.2}$, $S_{0.4}$, $S_{0.6}$, $S_{0.8}$ and S_1, respectively). Variation of saturation values with changing the Fe_3O_4 content

The surface compositions and the elemental chemical oxidation states were studies using XPS technique. The full survey spectrum of the GO and G/Fe3O4 nanocomposite was shown in Figure (4A). sharp peaks at binding energies of 284.8 and 531.6 related to (C 1s) and 531.6 (O 1s) respectively have been appeared as indication that the samples contain C and O elements. In addition to, G/Fe3O4 nanocomposite has characteristic peak at 711.48 eV (Fe 2p). The production of grapheme oxide by using Hammers method has been proved as shown in fig. (4B). The oxygen containing functional groups of the non-oxygenated carbon located at (C=C) at 284.6 eV, the C–O bond (epoxy and hydroxyl) at 286.7 eV and the carboxylate carbon (C=O) at 288.8 eV were observed Deng et al., [27]. For the C1s peak of G/Fe3O4 is well resolved in to three spectral components in the Fig. (4C), which are sp^2 C=C (at 284.8 eV), carbons in C-OH (at 286.2 eV) and carboxyl/epoxy C=O

(at 288.4 eV) . The DE convolution of C1s indicates that G/Fe3O4 consists of a main peak centered at 284.8 eV (sp^2 C=C), which represents the reduction of GO into G after solvothermal method.

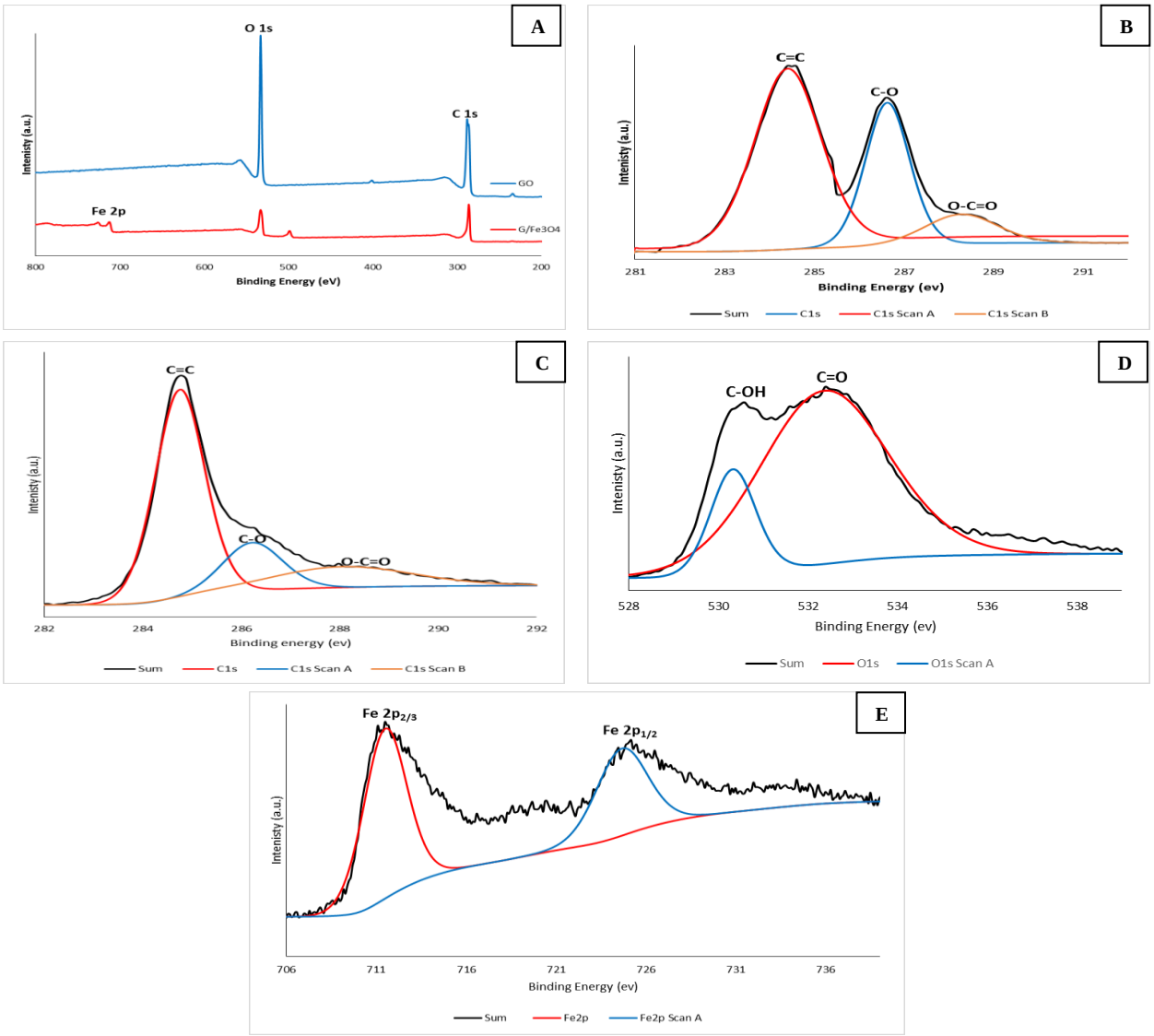

Figure 4. The survey XPS spectrum of GO and G/Fe3O4 (A),C 1sspectrum of GO (B), C 1s spectrum of G/Fe3O4 (C), O 1s spectrum of G/Fe3O4 (D) and Fe 2p spectrum of G/Fe3O4 (E).

The relative intensities of the peaks associated with oxygen-containing functional groups decreased sharply compared with peaks of GO. Suggesting that most of the oxygen functional groups (C-OH, C=O) have been successfully reduced [28,29]. For the O 1s region spectrum of G/Fe3O4 , the photoelectron can be resolved into two curves with peaks at binding energies 530.6 and 532.4 eV, which represent the binding energies of oxygen in the –OH and O^{-2} species, respectively Fig.(4D). Also, Fig.(4E), shows a Fe2p spectrum of G/Fe3O4. Distinct two peaks of an Fe2p level with binding energies at 711.5 and 725.7 eV were assigned to spin–orbit peaks Fe $2p_{3/2}$ and Fe $2p_{1/2}$ of Fe_3O_4 respectively, which indicate the formation of pure magnetite in the G/Fe3O4 nanocomposite [30].

Figure 5 shows the UV–vis absorption spectra of the GO, G, G/Fe3O4 . GO presented by characteristic peak at 229 nm corresponding to $\pi - \pi^*$ transitions of aromatic C–C bonds [105]. Red shift peak of the Graphene presented at 260 nm because the electronic conjugation in the graphene. While for G/Fe3O4 , the absorption peak was shifted to 268 nm, suggesting that the covalent attachment of Fe_3O_4 on to graphene surface.

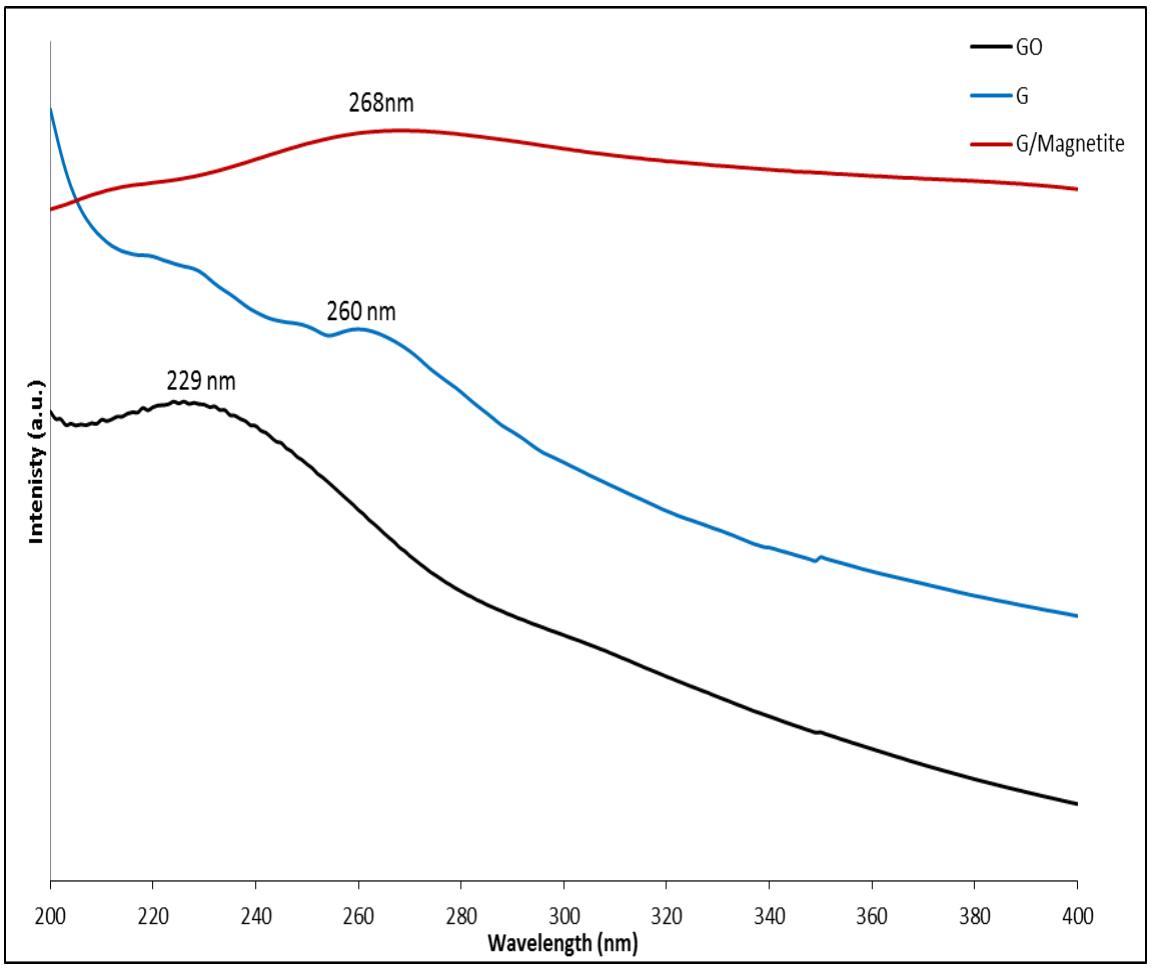

Figure 5.UV–vis absorption spectra of GO, G and G/Fe3O4

3.2 Adsorption work

As shown in Figure 6,the adsorption of MB on different ratios of G/ Fe_3O_4 nanocomposites (m Fe_3O_4: m GO = 0.1:1, 0.2:1, 0.4:1, 0.6:1, 0.8:1 and 1:1) was recorded. With the increasing the Fe_3O_4 NPs on the surface of the G sheet the adsorption capacity decreased due to the surface of the G sheet was occupied by Fe_3O_4 NPs. So the active sites of G sheet were blocked with Fe_3O_4 NPs, so the adsorption capacity decreased.

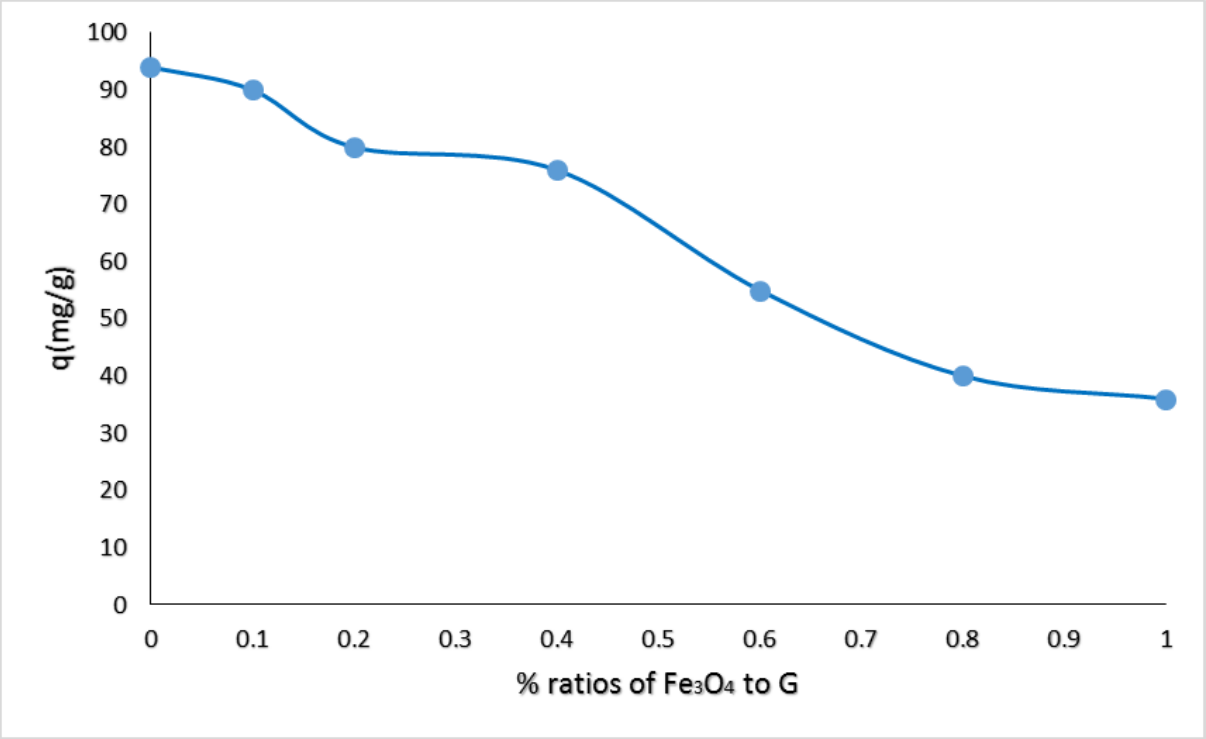

Figure 6. A dsorption of MB ondifferent ratios of pure Graphene and G/ Fe_3O_4 nanocomposites(different ratios: ($S_{0.1}$, $S_{0.2}$, $S_{0.4}$, $S_{0.6}$, $S_{0.8}$ and S_1, respectively).

4. CONCLUSION

In this study, we have prepared graphene/Fe_3O_4nanocomposites (G/Fe3O4) with different ratios by changing the feeding weight ratios of Fe_3O_4 to GO (m Fe_3O_4: m G = 0.1:1, 0.2:1, 0.4:1, 0.6:1, 0.8:1 and 1:1). Prepared nanocomposites characterized by a morphology of a uniform sheet like shape of prepared graphene and a uniform spherical homogeneously distributed of Fe_3O_4 Nps with no agglomeration over the graphene sheets. .Results also showed that, increasing the Fe_3O_4 NPs on the surface of the G sheet will lead to decrease the adsorption capacity. On the other hand, the magnetization has been increased sharply with increasing the Fe_3O_4Nps.

ACKNOWLEDGEMENTS
The authors would like to extend their sincere appreciation to the Deanship of Scientific Research at King Saud University for funding this research group NO. RG#1435-010. Also, we would like to thank the scientific research team at Nanotechnology and Advanced Materials Central Lab, Agriculture Research Center, Egypt, where all the experiments and characterization were done.

References

1. ATSDR, CERCLA Priority List of Hazardous Substances,http://www.atsdr.cdc. gov/cercla/07list.html(2007).
2. hanchang SHI, Industrial wastewater-types, amounts and effects, point sources of pollution: local effects and its control – Vol. I – industrial wastewater-types, amounts and effects – hanchang SHI

3. O. Ligrini, E. Oliveros, A. Braun, *Chem. Rev*. 93 (1993) 671.
4. U. Pagga, D. Brown, *Chemosphere* 15 (1986) 479.
5. J.M. Wang, C.P. Huang, H.E. Allen, et al. *J. Colloid Interf. Sci*. 208 (1998) 518.
6. K.M. Parida, S. Sahu, K.H. Reddy, P.C. Sahoo, *Ind. Eng. Chem. Res*. 50 (2011) 843.
7. T. Zhang, R. Surampalli , K. Lai, Z. Hu. Nanotechnologies for water environment applications. Amer Society of Civil Engineers. 2009.
8. Abdullah M. Al-Enizi, Ahmed A. Elzatahry, Mariam A. AlMaadeed, Jinxiu Wang, Dongyuan Zhao, Salem Al-Deyab ,Synthesis and electrochemical properties of nickel oxide/carbon nanofiber composites. CARBON, 2014, 71, 276-283.
9. R.S. Amin, A.A. Elzatahry, K.M. El-Khatib, M.E. Youssef - *Int. J. Electrochem. Sci*, 6 (2011) 4572-4580.
10. T. A. Salah El-Din, A. A. Elzatahry, D. M. Aldhayan, A. M. Al-Enizi and S. S. Al-Deyab. *Int. J. Electrochem. Sci.*, 6 (2011) 6177 – 6183.
11. Y. Wang, J. Tang, Z Peng, Y. Wang, D. Jia, B. Kong. *NanoLett*. 14 (2014) 3668−3673
12. T. Zhang , R. Surampalli, K. Lai, Z. Hu. Nanotechnologies for water environment applications. Amer Society of Civil Engineers. 2009.
13. Ahmed A. Elzatahry, Aboubakr M. Abdullah, Taher A. Salah El-Din, Abdullah M. Al-Enizi, Ahmed A. Maarouf , Ahmed Galal, Hagar K. Hassan, Ekram H. El-Ads, Salem S. Al-Theyab and Attiah A Al-Ghamdi, *Int. J. Electrochem. Sci*., 7 (2012) 3115 – 3126.
14. A. T. Lawal, *Talanta*, 131 (2015), 424–443.
15. M.H. Chakrabarti, C.T.J. Low, N.P. Brandon, V. Yufit, M.A. Hashim, M.F. Irfan, J. Akhtar, E. Ruiz-Trejo, M.A. Hussain, *Electrochimica Acta*, 107 (2-13) 425-440.
16. Y. Gao, Y. Li, L. Zhang, H. Huang, J. Hu, S.M. Shah, X. Su, , *J. Colloid Interface Sci*. 368 (2012) 540–546.
17. Y. Li, P. Zhang, Q. Du, X. Peng, T. Liu, Z. Wang, Y. Xia, W. Zhang, K. Wang, H. Zhu, D. Wu, *J. Colloid Interface Sci*. 363 (2011) 348–354.
18. S.T. Yang, S. Chen, Y. Chang, A. Cao, Y. Liu, H. Wang, *J. Colloid Interface Sci*. 359 (2011) 24–29.
19. Z. Geng, Y. Lin, X. Yu, Q. Shen, L. Ma, Z. Li, N. Pan, X. Wang, *J. Mater. Chem*. 22 (2012) 3527–3535.
20. G. Xie, P. Xi, H. Liu, F. Chen, L. Huang, Y. Shi, F. Hou, Z. Zeng, C. Shao, J. Wang, *J. Mater. Chem*. 22 (2012) 1033–1039.
21. Q. Wu, C. Feng, C. Wang, Z. Wang. *Colloids and Surfaces B: Biointerfaces*, 101 (2013) 210–214.
22. R. Wu, J. Liu, L. Zhao, X. Zhang, J. Xie, B. Yu, X. Ma, S. Yang, H. Wang, Y. Liu. *Journal of Environmental Chemical Engineering*, 2 (2014) 907-913.
23. L. Ai, C. Zhang, Z. Chen, *Journal of Hazardous Materials* 192 (2011) 1515–1524.
24. W.S. Hummers Jr., R. Offeman, *Journal of the American Chemical Society* 80 (1958) 1339.
25. L. Meng and S. Park, *Bull. Korean Chem. Soc*. 33 (2012) 209-214.
26. J. Deng, X. Zhang, G. Zeng, J.Gong, Q. YaNiu, J. Liang, , *Chemical Engineering Journal* 226 (2013) 189–200.
27. Q. Hana, Z. Wangb, J. Xiab, S. Chena, X. Zhanga, M. Dinga, *Talanta* 101 (2012) 388-395.
28. H. Sun, L. Cao, L. Lu, *Nano Res*. 4 (2011) 550–562.
29. V. Chandra, J. Park, Y. Chun, J.W. Lee, I.C. Hwang, K.S. Kim, *ACS Nano* 4 (2010) 3979–3986.
30. J. Lu, X.L. Jiao, D.R. Chen, W. Li, *Journal of Physical Chemistry* C 113(2009) 4012–4017